International Journal of Nanomedicine

Dovepress
open access to scientific and medical research

Open Access Full Text Article

ORIGINAL RESEARCH

Interaction of poly-L-lysine coating and heparan sulfate proteoglycan on magnetic nanoparticle uptake by tumor cells

This article was published in the following Dove Press journal:
International Journal of Nanomedicine

Wei Xiong Siow[1,2]
Yi-Ting Chang[1,2]
Michal Babič[3]
Yi-Ching Lu[2]
Daniel Horák[3]
Yunn-Hwa Ma[1,2,4]

[1]Graduate Institute of Biomedical Sciences, College of Medicine, Chang Gung University, Guishan, Taoyuan, Taiwan, Republic of China; [2]Department of Physiology and Pharmacology and Healthy Aging Research Center, College of Medicine, Chang Gung University, Guishan, Taoyuan, Taiwan, Republic of China; [3]Institute of Macromolecular Chemistry, Czech Academy of Sciences, Prague, Czech Republic; [4]Department of Neurology, Chang Gung Memorial Hospital, Guishan, Taoyuan, Taiwan, Republic of China

Background: Poly-L-lysine (PLL) enhances nanoparticle (NP) uptake, but the molecular mechanism remains unresolved. We asked whether PLL may interact with negatively charged glycoconjugates on the cell surface and facilitate uptake of magnetic NPs (MNPs) by tumor cells.
Methods: PLL-coated MNPs (PLL-MNPs) with positive and negative ζ-potential were prepared and characterized. Confocal and transmission electron microscopy was used to analyze cellular internalization of MNPs. A colorimetric iron assay was used to quantitate cell-associated MNPs (MNP_{cell}).
Results: Coadministration of PLL and dextran-coated MNPs in culture enhanced cellular internalization of MNPs, with increased vesicle size and numbers/cell. MNP_{cell} was increased by eight- to 12-fold in response to PLL in a concentration-dependent manner in human glioma and HeLa cells. However, the application of a magnetic field attenuated PLL-induced increase in MNP_{cell}. PLL-coating increased MNP_{cell} regardless of ζ-potential of PLL-MNPs, whereas magnetic force did not enhance MNP_{cell}. In contrast, epigallocatechin gallate and magnetic force synergistically enhanced PLL-MNP uptake. In addition, heparin, but not sialic acid, greatly reduced the enhancement effects of PLL; however, removal of heparan sulfate from heparan sulfate proteoglycans of the cell surface by heparinase III significantly reduced MNP_{cell}.
Conclusion: Our results suggest that PLL-heparan sulfate proteoglycan interaction may be the first step mediating PLL-MNP internalization by tumor cells. Given these results, PLL may facilitate NP interaction with tumor cells via a molecular mechanism shared by infection machinery of certain viruses.

Keywords: magnetic nanoparticles, poly-L-lysine, tea catechin, glycoconjugate, heparan sulfate proteoglycan

Introduction

Cellular internalization of nanoparticles (NPs) is an extensively studied area in an effort to improve targeting efficacy and understand distribution of the NPs in the body.[1,2] Superparamagnetic NPs have potential as carriers of pharmacological and biological agents in targeted delivery. Under external magnetic force, magnetic NPs (MNPs) can be manipulated and guided to a target site. Local retention of nanocomposites may prolong the half-life of the drug, enhance therapeutic efficacy, and reduce systemic adverse effects.[3–5] Application of a static magnetic field enhances MNP uptake by cultured cells, primarily by enhancing the sedimentation rate of MNPs.[6] The subsequent interaction between the cell and the NP is also important for cellular uptake, which may impact pharmacological efficacy. Specifically, the surface of MNPs can be modified to modulate uptake. For example, surface coating by polymers has been shown to confer targeting ability, colloidal stability, and/or multifunctionality.[7]

Correspondence: Yunn-Hwa Ma
Department of Physiology and Pharmacology, Chang Gung University, 259 Wen-Hwa 1st Road, Guishan, Taoyuan 33302, Taiwan, Republic of China
Tel +886 3 211 8800 ext 5152/5266
Fax +886 3 211 8700
Email yhma@mail.cgu.edu.tw

submit your manuscript | www.dovepress.com
Dovepress
http://dx.doi.org/10.2147/IJN.S156029

Various chemicals have been used to enhance cellular uptake of NPs, including poly-L-lysine (PLL), which is also applied to gene delivery[8–10] and cell labeling.[11–14] The addition of PLL to cultures enhances NP internalization by stem cells[15,16] and tumor cells.[16,17] PLL coating of NPs undergoes similar uptake enhancement in a variety of cells.[13,18–21] Although electrostatic interaction has been proposed,[11–13,15,17] the mechanism of PLL-induced internalization of NPs has not been elucidated.

PLL is a linear polymer of lysine that bears a positive charge at neutral pH, which can electrostatically interact with the negatively charged molecules at the cell surface.[22] Complex carbohydrates are primarily responsible for the net negative charge of the cell surface. These macromolecules are composed of one or more carbohydrate chains that commonly link to a protein or lipid and are conservatively located at the cell membrane as glycoconjugates.[23] In mammalian cells, the major types of glycoconjugates include glycoprotein, proteoglycan (PG), and glycosphingolipid. Most glycoproteins and glycosphingolipids in mammalian cells contain sialic acid residues, which impart a negative charge to the plasma membrane. PGs are proteins that contain glycosaminoglycan (GAG), and are classified into several types, including glypican, syndecan, and perlecan. GAG polysaccharides, such as heparan sulfate (HS), are highly anionic compounds, due to the presence of uronic acid and sulfates. GAGs are covalently linked to a core protein, and vary in tissue distribution and function.[24] A specific type of PG, HSPG is involved in several biological processes influencing cellular events, including signaling, migration, and tumor invasion.[24–26] In addition, an increasing number of reports indicate that HSPG on the cell surface mediates endocytosis,[27–30] especially in the virus-transduction pathway.[31,32] Previous studies have demonstrated that HIV invasion requires transactivator proteins with arginine- and lysine-rich regions for anchoring on cell-surface HSPG, which subsequently mediates the virus entry.[33–35] There is general agreement that binding to HSPG is a crucial step for internalization of cationic peptides and polymers, such as protein-transduction-domain or cell-penetrating peptides with high arginine density.[34,36] In addition, hepatitis B virus also interacts with HSPG as the first step of cell entry.[37] Despite the plausible electrostatic interaction mechanism, it is not known whether interaction of lysine-rich coating with HSPG is involved in NP internalization.

In addition to PLL, research has indicated that epigallocatechin-3-gallate (EGCG), a polyphenolic component in tea, enhances MNP internalization,[38] which is also negatively charged due to the presence of phenolic groups. Moreover, EGCG is a known antioxidant with antitumor and anti-inflammatory activities,[39–41] which are probably mediated by interaction with a 67 kDa laminin receptor.[42,43] However, the antioxidant activity of EGCG may be separate from its enhancement effect on MNP internalization by glioma cells.[38]

In this study, we asked whether PLL interacts electrostatically with negatively charged residues of glycoconjugates on the surface of glioma cells to enhance NP uptake. Since vascular endothelial cells are often exposed to NPs in circulation after parenteral delivery, effects of PLL on MNP uptake by endothelial and glioma cells were compared. We found that PLL coating interacted with negatively charged residues of HSPG, which may impact the magnetic sensitivity of MNP uptake.

Materials and methods

Chemicals

Dextran (Dex)-coated magnetite NPs (nanomag®-D, 250 nm, subsequently denoted "Dex-MNPs") containing carboxyl groups for drug immobilization were obtained from Micromod Partikeltechnologie GmbH (Rostock, Germany), and Dex-MNPs conjugated with a green fluorophore were obtained from Chemicell GmbH (Berlin, Germany). $FeCl_2 \cdot 4H_2O$ and $FeCl_3 \cdot 6H_2O$ were purchased from Fluka (Buchs, Switzerland), sodium hypochlorite solution (NaOCl) from Bochemie (Bohumín, Czech Republic), and sodium citrate dihydrate was obtained from Lachema (Brno, Czech Republic). All other reagent-grade chemicals were purchased from Sigma-Aldrich (St Louis, MO, USA) and used as received. DMEM and MEM were purchased from Thermo Fisher Scientific (Waltham, MA, USA). Penicillin–streptomycin–amphotericin B was purchased from Upstate Biotechnology (Lake Placid, NY, USA). Fetal bovine serum (FBS) was purchased from SAFC Biosciences (Lenexa, KS, USA). Endothelial cell-growth supplement was purchased from Merck Millipore (Billerica, MA, USA). PLL hydrobromide (M_w 93,800 Da as coating material and M_w 388,100 Da for incubation of Dex-MNPs), ammonium persulfate, potassium thiocyanate, heparin (Hep) sodium salt from porcine intestinal mucosa (grade IA), EGCG, Bovine serum albumin (BSA), paraformaldehyde (PFA), dimethyl sulfoxide, sodium chloride (NaCl), potassium chloride (KCl), sodium phosphate dibasic, potassium dihydrogen phosphate, and heparinase III from *Flavobacterium heparinum* (EC 4228) were from Sigma-Aldrich. Components of Epon mixture were purchased from Nacalai Tesque (Kyoto, Japan). Uranyl acetate was purchased from SPI Supplies (West Chester, PA, USA). Wheat-germ agglutinin (WGA) and 4′,6-diamidino-2-phenylindole (DAPI) were purchased from Thermo Fisher Scientific. Ultrapure Q water ultrafiltered on a Milli-Q Gradient A10 system (Merck Millipore) was used for the preparation of solutions.

Synthesis of magnetic nanoparticles

An aqueous 0.2 M $FeCl_3$ solution (12 mL) was mixed with 0.5 M NH_4OH solution (12 mL, less than an equimolar amount) at room temperature under sonication (Sonicator W-385; Sonicator, Farmingdale, NY, USA) for 2 minutes to form $Fe(OH)_3$ colloid. Aqueous 0.2 M $FeCl_2$ (6 mL) was added to the colloid under sonication, and the mixture was poured into 0.5 M NH_4OH aqueous solution (36 mL) under argon atmosphere. The resulting magnetite (Fe_3O_4) coagulate was left to grow for 45 minutes, magnetically separated, and washed seven times (peptized) with Milli-Q water to remove all impurities, including NH_4Cl, remaining after the synthesis. Then, 0.1 M sodium citrate (1.5 mL) or 0.1 M HCl (2.2 mL) was added under sonication and the magnetite oxidized by the slow addition of 5% sodium hypochlorite solution (1 mL) to maghemite (γ-Fe_2O_3) to enhance redox stability. The washing procedure was repeated to yield the primary colloid, denoted as MNP^- and MNP^+. Aqueous PLL solution (0.2 mL; 1 mg/mL) was added dropwise with stirring to the primary colloid (10 mL) and the mixture diluted to a concentration of 4.4 or 10 mg of iron oxide. The resulting mixture was sonicated for 5 minutes before use.

Particle characterization

The morphology of the colloids was characterized by transmission electron microscopy (TEM; JEM 200 CX; JEOL, Tokyo, Japan). Particle-size distribution was obtained using Atlas imaging software (Tescan, Brno, Czech Republic). For the measurements, a drop of a dilute dispersion was spread on a carbon-coated copper grid, and the grid was air-dried at room temperature. Particle-size distribution of the nearly spherical particles was determined by the measurement of at least 700 particles for each sample. Two types of mean particle size were calculated: the number-average particle size (D_n) and the weight-average particle size (D_w; $D_n = \sum D_i/n$ and $D_w = \sum D_i^4/\sum D_i^3$, where n is the number of particles). Particle-size distribution was characterized by the polydispersity index (PDI; D_w/D_n). Moreover, hydrodynamic diameter (z-average), polydispersity (PI from 0 [monodisperse particles] to 1 [polydisperse particles]) from cumulative analysis of time-correlation function, and surface ζ-potential were determined by dynamic light scattering (DLS) using an Autosizer Lo-C (Malvern Instruments, Malvern, UK).

Cell culture

Cells from the Food Industry Research and Development Institute (Taiwan) were cultured and maintained as previously described.[38] Briefly, human glioma cell lines LN229 and U87MG were maintained in DMEM and MEM, respectively. Both culture media contained 10% FBS and 1% penicillin–streptomycin–amphotericin mixture. Human umbilical vein endothelial cells (HUVECs) were isolated from human umbilical cords with a procedure approved by the institutional review board of Chang Gung Memorial Hospital to study the interaction of MNPs and HUVECs, with written informed consent obtained from the patients for the use of the HUVECs for research. HUVECs were maintained in M199 medium containing 10% FBS, endothelial cell-growth supplement (30 µg/mL), 1% penicillin–streptomycin–amphotericin B mixture, and Hep (20 U/mL). In experiments that assessed the effect of Hep, Hep was not added to the culture medium. Cells were maintained in an incubator at 37°C under a 5% CO_2 atmosphere and used from passages two to ten. When heparinase III was used for pretreatment of cells, the enzyme was reconstituted in a lyase buffer (20 mM Tris-HCl, 0.1 mg/mL BSA, and 4 mM $CaCl_2$) and diluted by digestion buffer (MEM supplemented with 0.5% w/v BSA and 20 mM of HEPES) in pH 7.5, as previously described.[44] Cells were incubated with 5 mIU/mL of heparinase III for 3 hours, followed by incubation with 100 µg/mL of PLL-MNP^+ for 1 hour prior to the iron assay.

Confocal microscopy

Cells were seeded on coverslips 8 hours before experiments. After reaching ~60%–70% confluence, cells were incubated with Dex-MNPs conjugated with a green fluorophore (100 µg/mL, Ex/Em 488/490 nm), and PLL (3 nM) at 37°C for 1 hour. Additionally, a homemade magnetic plate (~3.4 kG) was placed underneath the 24-well culture plate for 5 minutes to facilitate sedimentation, as previously described.[6] Cells were rinsed with PBS twice, fixed with 4% PFA for 20 minutes, incubated with 0.2% BSA (blocking agent) for 0.5 hours three times, and counterstained. Extracellular glycoproteins and nuclei were counterstained with WGA (5 µg/mL, Ex/Em 633/647 nm) and DAPI (300 nM, Ex/Em 405/470), respectively, for 20 minutes each. Cells were monitored by confocal laser microscopy (LSM 510 Meta; Carl Zeiss Meditec, Jena, Germany) fitted with a 100×/1.4 oil-immersion objective lens.

Transmission electron microscopy

U87MG cells were seeded in 24-well plate with plastic coverslips (Thermo Fisher Scientific) to ~10^6 cells/well and incubated with MNPs (100 µg/mL). An NdFeB magnet was placed underneath the plate for 5 minutes to facilitate sedimentation. After incubation, the medium with MNPs was removed and the cells were gently washed with phosphate buffered saline (PBS; 137 mM NaCl, 2.7 mM KCl, 12 mM phosphate).

Incubation of a mixture of 3% (w/v) glutaraldehyde and 2% (w/v) PFA in 0.1 M cacodylate buffer (pH 7.4) at 4°C for 2 hours was used to fix the cells. The mixture was subsequently replaced by 1% osmium tetroxide for 1 hour. Cells were dehydrated in graded ethanol and embedded in Epon resin. Sections with 80 nm thickness were obtained, counterstained with 4% uranyl acetate in hydrogen peroxide for 2 hours and 0.4% lead citrate for 10 minutes, and were examined with TEM (H-7500; Hitachi, Tokyo, Japan) at Department of Anatomic Pathology, Chang Gung Memorial Hospital, Linkou.

Iron assay for MNP–cell interaction

Cells were cultured in a 24-well culture plate to 80%–90% confluence, which was followed by incubation with MNPs (100 μg/mL), EGCG (0–20 μM), PLL (0–30 nM), and/or Hep (0.1–10 U/mL). Experiments were conducted for 2–3 hours in the absence or presence of the homemade NdFeB magnet array (~3.4 kG), as described previously.[6] Cells were trypsinized and treated with 10% hydrochloric acid at 55°C for 4 hours, after which ammonium persulfate (1 mg/mL) and potassium thiocyanate (1 M) were added. The amount of iron in the MNPs was determined with a VICTOR3 Multilabel Plate Reader (PerkinElmer, Shelton, CT, USA) at OD_{490} using a calibration curve. Iron measurement represented cell-associated MNPs (MNP_{cell}), and included MNPs on the surfaces of cells that had not been removed during the process plus MNPs that had been internalized by cells during treatment.

Statistical analysis

Values are means ± SE unless otherwise stated. Student's *t*-test was used to analyze comparisons between paired values. In contrast, analysis of variance was used to analyze multiple results, followed by Duncan's post hoc test for individual comparison. The significance level for this study was $P<0.05$.

Results

Characterization of MNPs

Surface modification of MNPs based on iron oxides is a general strategy for enhancing both colloidal stability and engulfment by the cells. The most widely used iron oxide NPs, which are approved by the US Food and Drug Administration as a contrast agent for magnetic resonance imaging, are Dex-MNPs. These particles were also investigated in this report, and the results compared with those obtained on synthesized maghemite NPs. Stable dispersions of the latter particles were obtained by adsorbing negatively charged citrate ions (MNP^-) or positively charged hydroxonium ions (MNP^+). Properties of the magnetic particles are given in Table 1. TEM analysis indicated that the dry $MNPs^-$ and $MNPs^+$ had rather narrow particle size distribution characterized by PDI ~1.2 (Figure 1A and C). The number-average size of the NPs was ~10 nm (Table 1). The colloids showed high stability at neutral pH, with no sedimentation observed even after 2-month storage. NP stability can be ascribed to their small size and high absolute ζ-potential values (−56 or 57 mV).

NPs transport in cells can be dramatically altered through the attachment of peptides. Here, NP surfaces were modified by PLL (M_w 93,800 Da). Consistent with past findings,[13] postsynthesis coating of the primary iron oxide colloid with PLL did not change the morphology or the size of the iron oxide crystallites (Table 1; Figure 1B and D). Unremarkably, Table 1 shows that the hydrodynamic particle diameter of PLL-MNPs (~79 nm) measured by DLS was substantially larger than that obtained by TEM. In part, statistical diameters differ (intensity vs number-weighted mean diameter) and TEM provides the size of dry particles, whereas size by DLS includes the hydration layer. Both measures had low polydispersity values (PI ~0.15).

PLL enhanced MNP internalization by tumor cells

For cell uptake, Figure 2 shows enhanced internalization of Dex-MNPs by U87MGs with PLL treatment. Fluorescent Dex-MNPs were localized primarily in the cytosol of U87MG cells without entering the nucleus (Figure 2A and B). Based on the confocal images, PLL treatment resulted in fluorescence intensity that was 3.4-fold higher relative to

Table 1 Characteristics of MNPs

MNPs	Polymer	D_n, nm (TEM)	PDI (TEM)	D_h, nm (DLS)	PI (DLS)	ζ-Potential (mV)	pH
Dex-MNPs[a]	Dex			263.7±5.5		−40.1±0.3	
$MNPs^-$	–	9.7	1.22	79.3±0.1	0.124±0.02	−56±2	8.25
PLL-$MNPs^-$	PLL	10.1	1.19	119±3	0.25±0.02	−47±1	7.9
$MNPs^+$	–	9.6	1.23	70.7±0.3	0.123±0.004	57±4	4.09
PLL-$MNPs^+$	PLL	10.2	1.19	69±2	0.145±0.006	61±1	4.13

Notes: [a]According to our previous study.[38] Values are presented as mean ± SD.

Abbreviations: MNPs, magnetic nanoparticles; Dex, dextran; PLL, poly-L-lysine; D_n, number-average diameter; TEM, transmission electron microscopy; PDI, polydispersity index; D_h, hydrodynamic diameter; PI, polydispersity; DLS, dynamic light scattering; MNP^-, MNPs with negative ζ-potential; MNP^+, MNPs with positive ζ-potential.

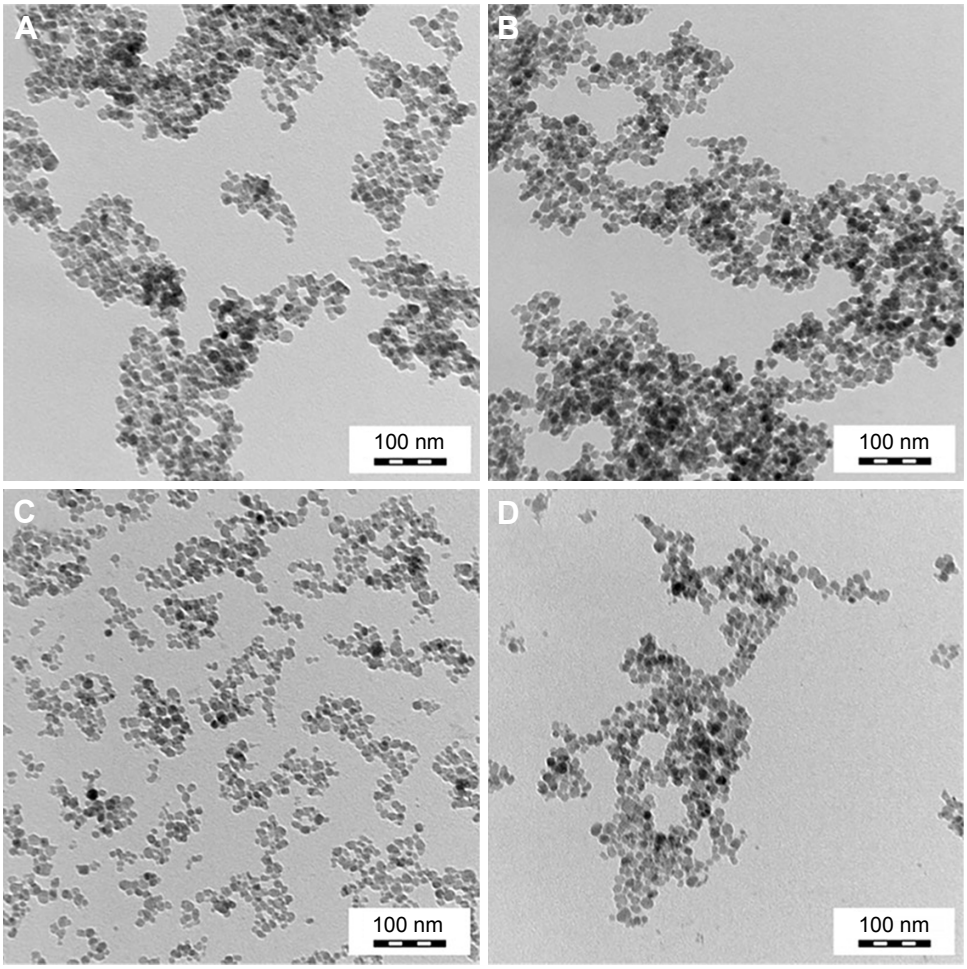

Figure 1 TEM of (**A**) $MNPs^{-}$, (**B**) PLL-$MNPs^{-}$, (**C**) $MNPs^{+}$, and (**D**) PLL-$MNPs^{+}$.
Abbreviations: TEM, transmission electron microscopy; MNPs, magnetic nanoparticles; PLL, poly-L-lysine; MNP^{-}, MNPs with negative ζ-potential; MNP^{+}, MNPs with positive ζ-potential.

the control (Figure 2E). After 24-hour incubation with PLL, MNPs were observed in vesicles located in the cytoplasm, but not nucleus, as shown in the TEM images (Figure 2C and D). From image analysis, vesicle size (Figure 2F) and numbers of vesicles/cell (Figure 2G) were both greater in the presence of PLL. In contrast to expectations, the application of magnetic force in the presence of PLL significantly reduced vesicle size and vesicle numbers/cell.

Dex-MNPs and PLL of various concentrations were coincubated with cells for 2 hours before the assay, and no significant cytotoxicity or morphology change was observed within the range of the concentrations studied (data not shown). In response to increased PLL concentration, MNP_{cell} peaked at PLL of 3–10 nM in U87MG (Figure 3A), LN229 (Figure 3B), and HeLa cells (Figure 3C), respectively, suggesting that PLL acts in a similar manner among distinct tumor cells. At 3 nM PLL, MNP_{cell} increased to 9.2-, 8.5-, and 12-fold that of control in U87MG, LN229, and HeLa cells, respectively. Here again, application of a magnetic field resulted in fewer tumor-cell-associated MNPs and MNP_{cell}. At 10–30 and 1–30 nM PLL, the magnetic field significantly reduced MNP_{cell} in U87MG and LN229 cells, respectively. Similar magnetic insensitivity was also observed in HeLa cells. Unlike PLL, EGCG and magnetic force exerted a synergistic effect on MNP internalization by U87MG cells, as illustrated in Figure 3D. At 10 μM EGCG, the magnetic force increased MNP_{cell} by 3.1-fold, suggesting that the enhancing effect of EGCG is very sensitive to magnetic fields. Similar effects of EGCG have also been observed in LN229 cells.[38]

Temperature sensitivity of MNP_{cell} induced by PLL

U87MG cells were incubated with MNPs and PLL under 37°C vs 4°C for 3 hours.[38,45] Low temperature significantly reduced MNP_{cell} of Dex-MNPs with and without free PLL by 36% and 74%, respectively, suggesting a temperature-dependent component of MNP_{cell} (Figure 4). At 4°C, free PLL enhanced cell-associated Dex-MNPs by a factor of

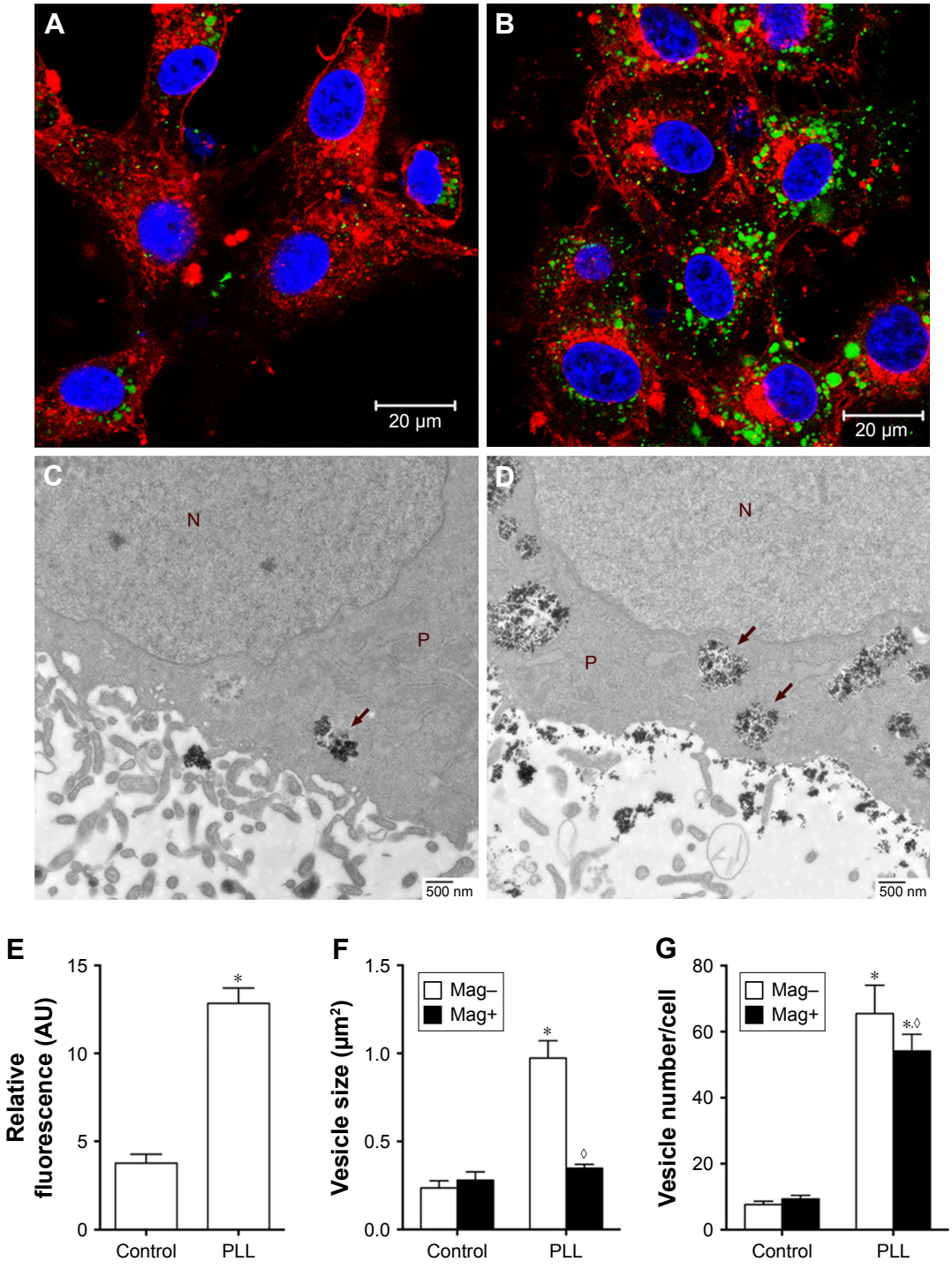

Figure 2 Enhancing effects of PLL on Dex-MNP internalization in U87MGs.

Notes: Representative (**A**, **B**) confocal and (**C**, **D**) TEM images in the absence (**A**, **C**) and presence (**B**, **D**) of 3 nM PLL for 1 and 24 h, respectively. (**A**, **B**) Cells counterstained with WGA (red) and DAPI (blue) after incubation with Dex-MNPs (green). (**C**, **D**) Internalized particles located in vesicles, as indicated by arrows. (**E**) Internalization of Dex-MNPs was quantitated based on fluorescence intensity, whereas (**F**) vesicle size and (**G**) vesicle numbers were analyzed from six to eight cells in each group with (Mag+) or without (Mag–) magnetic influence. $^{*,\lozenge}P<0.05$ compared with control and Mag– groups, respectively. N, nucleus; P, cytoplasm.

Abbreviations: PLL, poly-L-lysine; Dex, dextran; MNPs, magnetic nanoparticles; TEM, transmission electron microscopy; MNP^{-}, MNPs with negative ζ-potential; MNP^{+}, MNPs with positive ζ-potential.

10 relative to that in the absence of PLL, suggesting that PLL enhanced MNP–cell-surface interaction, but not endocytosis. At 4°C, cell-associated PLL-MNPs remained at similar levels irrespective of positive or negative ζ-potential, which were nine- to ten-fold that of MNPs without PLL coating. These results suggested that PLL-coating increased MNP_{cell} primarily via interacting with cell surfaces instead of energy-dependent endocytosis.

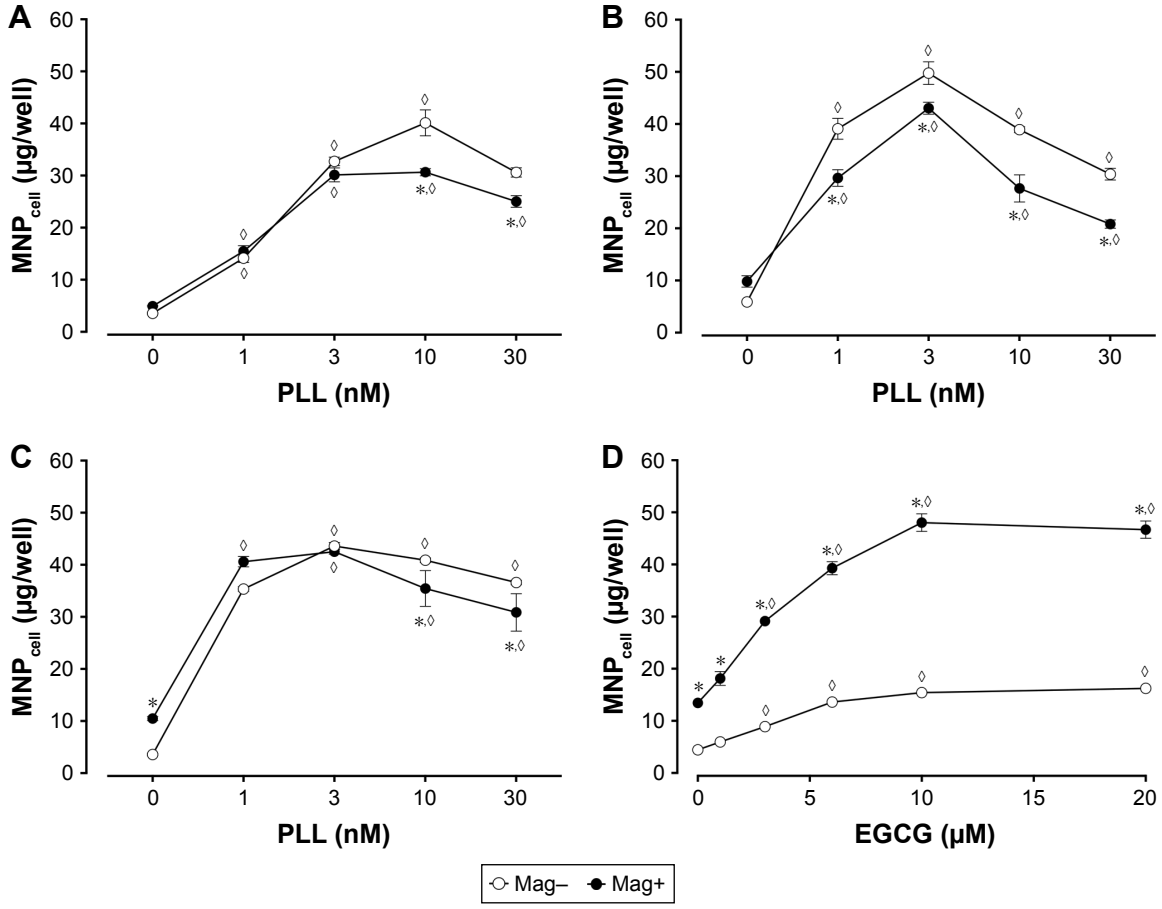

Figure 3 Effects of magnet on MNP_{cell} in (**A**, **D**) U87MGs (**B**) LN229, and (**C**) HeLa cells with (**A**–**C**) PLL or (**D**) EGCG.
Notes: Cells were incubated with Dex-MNPs for (**A**, **B**) 2 or (**C**, **D**) 3 hours with the magnet placed underneath (Mag+). In the Mag– group, the magnet was applied for 5 minutes to facilitate sedimentation of MNPs. Values are means ± SE (n=3). *,◊$P<0.05$ compared with Mag- and absence of PLL/EGCG, respectively.
Abbreviations: MNP_{cell}, cell-associated magnetic nanoparticles; Dex, dextran; PLL, poly-L-lysine; EGCG, epigallocatechin-3-gallate.

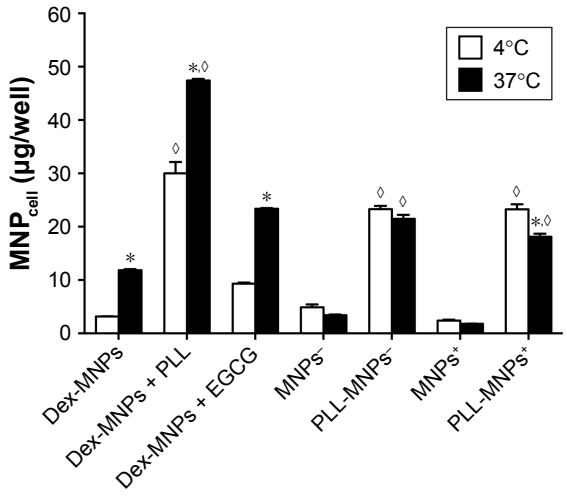

Figure 4 Temperature-dependent and independent components of MNP_{cell}.
Notes: U87MG cells were incubated with Dex-MNPs or PLL-MNPs (100 µg/mL) at 4°C or 37°C. In some groups, Dex-MNPs were coincubated with PLL (3 nM) or EGCG (10 µM). Values are means ± SE (n=3). *,◊$P<0.05$ compared with corresponding groups at 4°C without magnetic influence and control groups, respectively.
Abbreviations: MNP_{cell}, cell-associated magnetic nanoparticles; Dex, dextran; EGCG, epigallocatechin-3-gallate; MNP^-, MNPs with negative ζ-potential; MNP^+, MNPs with positive ζ-potential; PLL, poly-L-lysine.

Coincubation of PLL and MNPs

To determine the effect of PLL on the physiological function of the cells leading to the enhancement of MNP_{cell}, PLL was preincubated with the U87MG cells, followed by removal of PLL before addition of Dex-MNPs. Presence or absence of PLL during incubation of Dex-MNPs with cells is denoted in Figure 4 as PLL+/+ or PLL+/–, respectively. Moreover, Dex-MNPs premixed with or without PLL prior to their addition to the cells were denoted as PLL/MNP^+ and PLL/MNP^-, respectively. Figure 5A illustrates that incubation of 3 nM PLL with Dex-MNPs (PLL–/+, PLL/MNP^+) significantly increased MNP_{cell} by 9.2- and 2.9-fold in the absence (Mag–) or presence of the magnetic field (Mag+), respectively, compared to experiments without PLL. However, preexposure of cells with PLL followed by its removal from the medium during 24-hour incubation significantly reduced the effect of PLL at both 3 (Figure 5A) and 10 nM PLL (Figure 5B). In Mag– and Mag+ experiments lasting 24 hours, preincubation of 3 nM PLL and Dex-MNPs (PLL+/+, PLL/MNP^+)

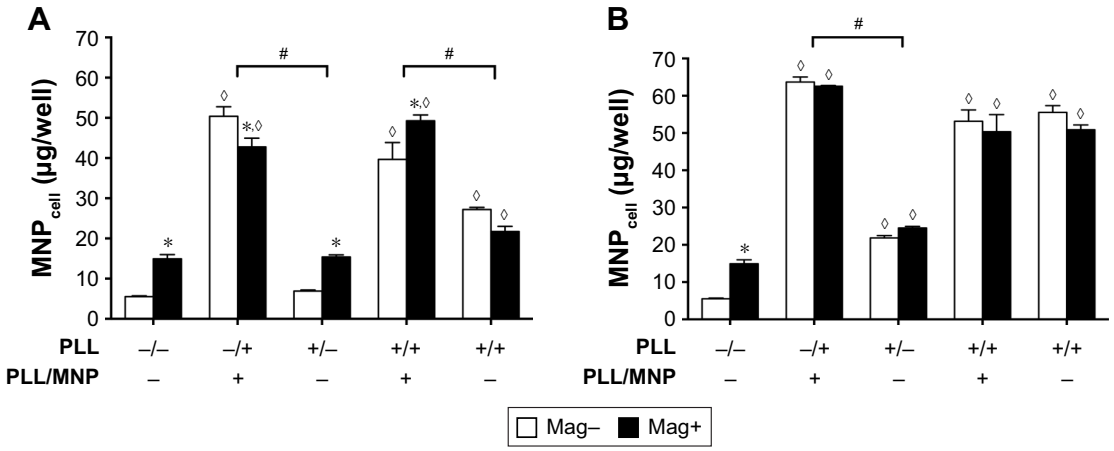

Figure 5 Coexistence of PLL and Dex-MNPs required for enhancement effects of PLL.
Notes: PLL (3 nM [**A**]; 10 nM [**B**]) was added to U87MG cells during incubation with Dex-MNPs. A magnetic field was applied for 5 minutes (Mag–) and 24 hours (Mag+) before or during 24-hour incubation, respectively. Preincubation of the cells with (+/–) or without (–/–) PLL for 1 hour was followed by 24-hour incubation with Dex-MNPs in the absence of PLL; preincubation of the cells with (+/+) or without (–/+) PLL for 1 hour was followed by 24-hour incubation with Dex-MNPs in the presence of PLL. In some experiments, PLL and MNPs were premixed for 1 hour before addition to the medium (PLL/MNP$^+$). Values are means ± SE (n=4). $^{*,\lozenge}P<0.05$ compared with Mag– and Dex-MNP alone, respectively; $^{\#}P<0.05$ for comparisons indicated.
Abbreviations: PLL, poly-L-lysine; Dex, dextran; MNPs, magnetic nanoparticles; MNP_{cell}, cell-associated MNPs; MNP^-, MNPs with negative ζ-potential; MNP^+, MNPs with positive ζ-potential.

prior to addition of particles in culture significantly increased MNP_{cell} to 7.2- and 3.3-fold, respectively, compared to those without PLL. However, significantly higher MNP internalization was observed with preincubation with 3 nM PLL, but not 10 nM PLL (Figure 5B).

PLL attenuated the effect of magnetic force

Since preincubation of PLL with Dex-MNPs enhanced Dex-MNP uptake by glioma cells, uptake of PLL-MNP^- and PLL-MNP^+ was determined. In the absence of the magnetic field (Figure 6A), MNP^- and PLL-MNP^+ increased MNP_{cell} by 11.5-fold and 3.8-fold in U87MG cells compared with neat MNP^- and MNP^+, respectively. Similar results were observed in LN229, except that PLL coating with positive ζ-potential appeared to be more potent than that with negative ζ-potential in LN229 cells (Figure 6B). However, magnetic force did not affect PLL-MNP uptake in either cell line (Figure 6). Without the magnet, EGCG (10 µM) reduced PLL-MNP^- internalization by 76% and 46% of that in U87MG and LN229 cells without EGCG, respectively (Figure 6), but EGCG did not affect uptake of MNPs without PLL coating. In contrast,

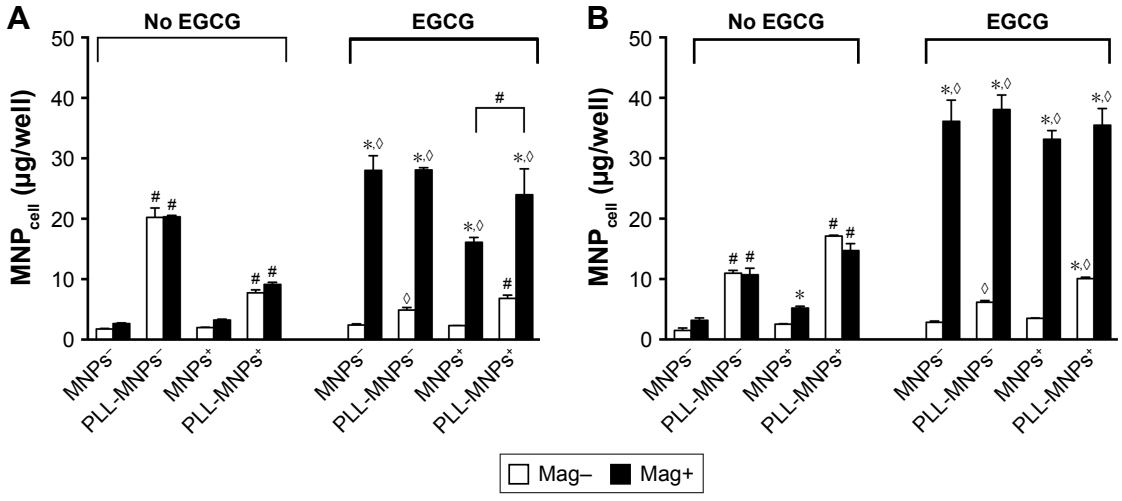

Figure 6 Synergistic effects of magnetic force and EGCG on internalization of MNPs with or without PLL coating by (**A**) U87MG and (**B**) LN229 cells.
Notes: Cells were incubated with EGCG (10 µM) and MNPs (100 µg/mL) for 3 hours. Values are means ± SE (n=4). $^{*,\lozenge}P<0.05$ compared with Mag– and no EGCG groups, respectively; $^{\#}P<0.05$ compared with corresponding MNPs without PLL coating.
Abbreviations: EGCG, epigallocatechin-3-gallate; MNPs, magnetic nanoparticles; PLL, poly-L-lysine; MNP^-, MNPs with negative ζ-potential; MNP_{cell}, cell-associated MNPs; MNP^+, MNPs with positive ζ-potential.

EGCG increased MNP_{cell} for all MNPs in the presence of the magnet. It is suggested that PLL enhanced cellular uptake due to positively charged amino groups, which were then abrogated by the hydroxyl groups of EGCG. However, it is noticeable that the magnetic field and EGCG had a remarkably synergistic effect on enhancing MNP internalization by both U87MG and LN229 cells.

Heparin and cleavage of heparan sulfate reduced tumor MNP_{cell}

To determine whether glycoconjugates on plasma membrane interacted with PLL and mediated the effects of PLL, anionic compounds mimicking glycoconjugate components were administered. Figure 7A and C illustrates that Hep decreased PLL-induced Dex-MNP uptake by U87MG and LN229 cells in a concentration-dependent manner. Hep at 1 U/mL reduced MNP uptake by 49% and 37% in the absence and presence of the magnet, respectively (Figure 7A). Similar effects of Hep were observed with PLL-MNP^- and PLL-MNP^+ (Figure 7B and D). Additionally, in order to eliminate surface HSPG, U87MG cells were pretreated with 5 mIU/mL of heparinase III for 3 hours prior to 1-hour incubation of PLL-MNPs. Figure 7 insert illustrates that MNP_{cell} of the PLL-MNP^+ was significantly decreased by 68% after depletion of

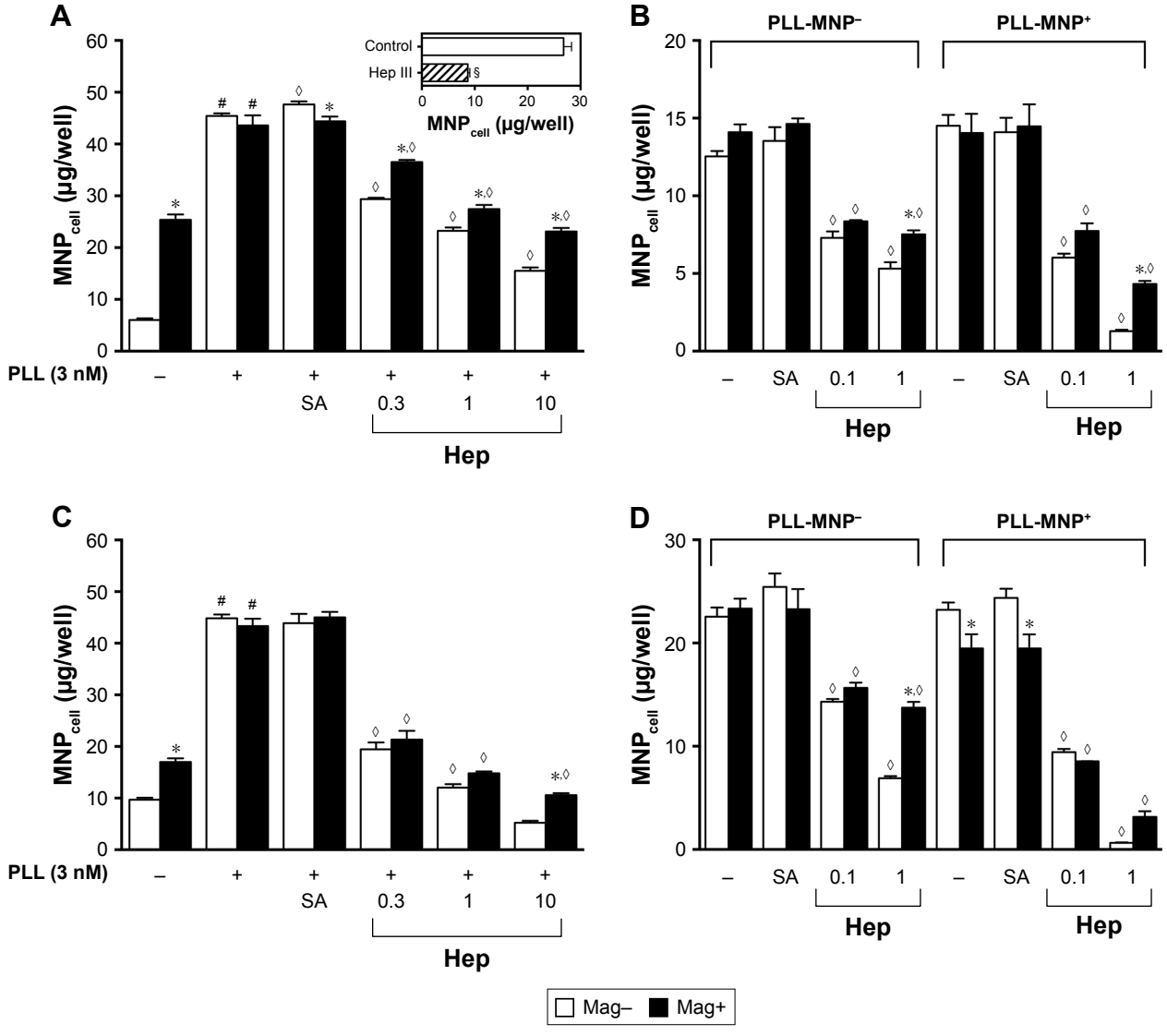

Figure 7 Heparin (Hep) attenuated the enhancing effects of (**A**, **C**) PLL and (**B**, **D**) PLL coating on internalization of (**A**, **C**) Dex-MNPs and (**B**, **D**) PLL-MNPs, respectively.
Notes: A magnetic field was applied for 5 minutes (Mag–) or 3 hours (Mag+) during the 3-hour incubation of Hep (0.1–10 IU/mL) or sialic acid (SA; 100 μM) with (**A**, **B**) U87MG or (**C**, **D**) LN229 cells. In some experiments, U87MG cells were incubated with 5 mIU/mL of heparinase III (Hep III) for 3 hours prior to PLL-MNP^+ treatment (**A** insert). Values are means ± SE (n=4). $^{*,\lozenge}P<0.05$ compared with Mag– and Hep–/PLL+, respectively. $^{\#,\S}P<0.05$ compared with corresponding PLL– group and control group, respectively.
Abbreviations: PLL, poly(L-lysine); Dex, dextran; MNPs, magnetic nanoparticles; MNP_{cell}, cell-associated MNPs; PLL-MNP^-, PLL-coated MNPs with negative ζ-potential; MNP^-, MNPs with negative ζ-potential; MNP^+, MNPs with positive ζ-potential; SA, sialic acid.

HS on cell surfaces compared to that of the control groups. In contrast, sialic acid (100 μM) exerted no effect on MNP_{cell}. These results suggest that PLL interacts with HS on the plasma membrane of the glioma cells.

PLL exerted minor effect on HUVEC MNP_{cell}

To determine whether PLL-mediated enhancement effects were specific to tumor cells, the effects of PLL on endothelial cells from primary culture were studied. Figure 8A illustrates that HUVEC-associated Dex-MNPs were significantly enhanced by the magnet, but not by PLL at any concentration studied. However, after removal of Hep from the culture medium, PLL exerted restored enhancement effects on MNP_{cell} (Figure 8B), which were concentration-dependent. Although levels of MNP_{cell} remained relatively low compared to those in tumor cells, PLL significantly increased MNP_{cell} by 6.1- and 1.7-fold compared with control groups in the absence or presence of the magnetic force, respectively. Similarly to the aforementioned results, the magnet exerted no enhancement effect of MNP_{cell} with PLL ≥3 nM. In the presence of Hep, only PLL-MNP^{-} increased MNP_{cell} in the absence of the magnet (by 2.7-fold) compared with the corresponding control group, as illustrated in Figure 8C. Nevertheless, magnetic force enhanced HUVEC-associated PLL-MNPs with (Figure 8C) or without (Figure 8D) Hep.

Discussion

Understanding the interaction between carriers and the plasma membrane of cells is crucial for optimizing delivery efficacy. In this study, we demonstrated that PLL interacts with MNPs and negatively charged moieties on the cell surface to facilitate MNP–cell interaction. Our results support HSPG serving as an endocytosis receptor for PLL-coated

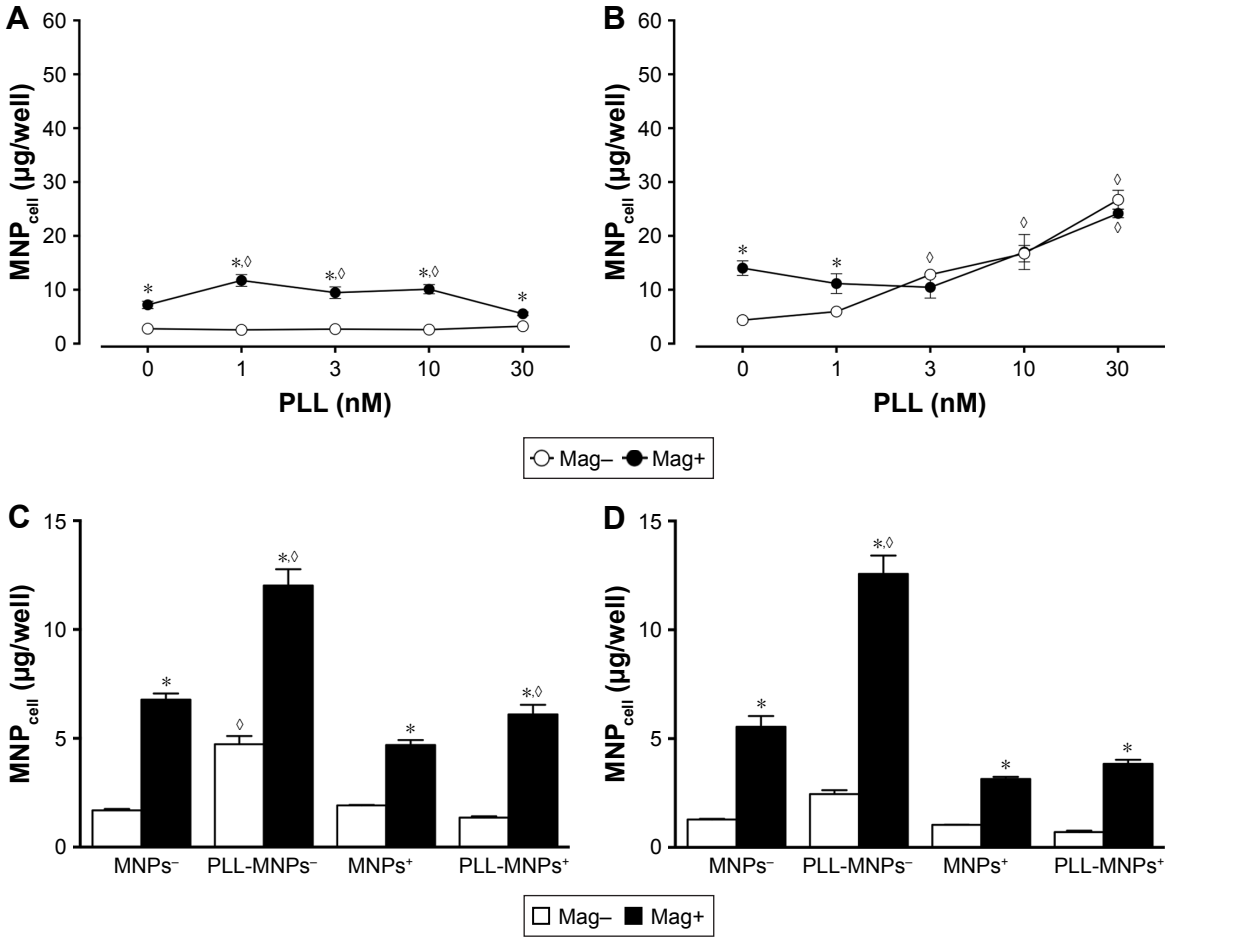

Figure 8 Magnetic force increased human umbilical-vein endothelial cell-associated (**A**, **B**) Dex-MNPs or (**C**, **D**) PLL-MNPs with or without heparin after 3-hour incubation.
Notes: A magnetic field was applied for 5 minutes (Mag–) or 3 hours (Mag+) in the (**A**, **C**) presence and (**B**, **D**) absence of heparin (20 IU/mL). Values are means ± SE (n=4). *,◊$P<0.05$ compared with Mag– and corresponding groups without PLL, respectively.
Abbreviations: Dex, dextran; MNPs, magnetic nanoparticles; PLL, poly-L-lysine; MNP_{cell}, cell-associated MNPs; MNP^{-}, MNPs with negative ζ-potential; MNP^{+}, MNPs with positive ζ-potential; PLL-MNP^{-}, PLL-coated MNPs with negative ζ-potential.

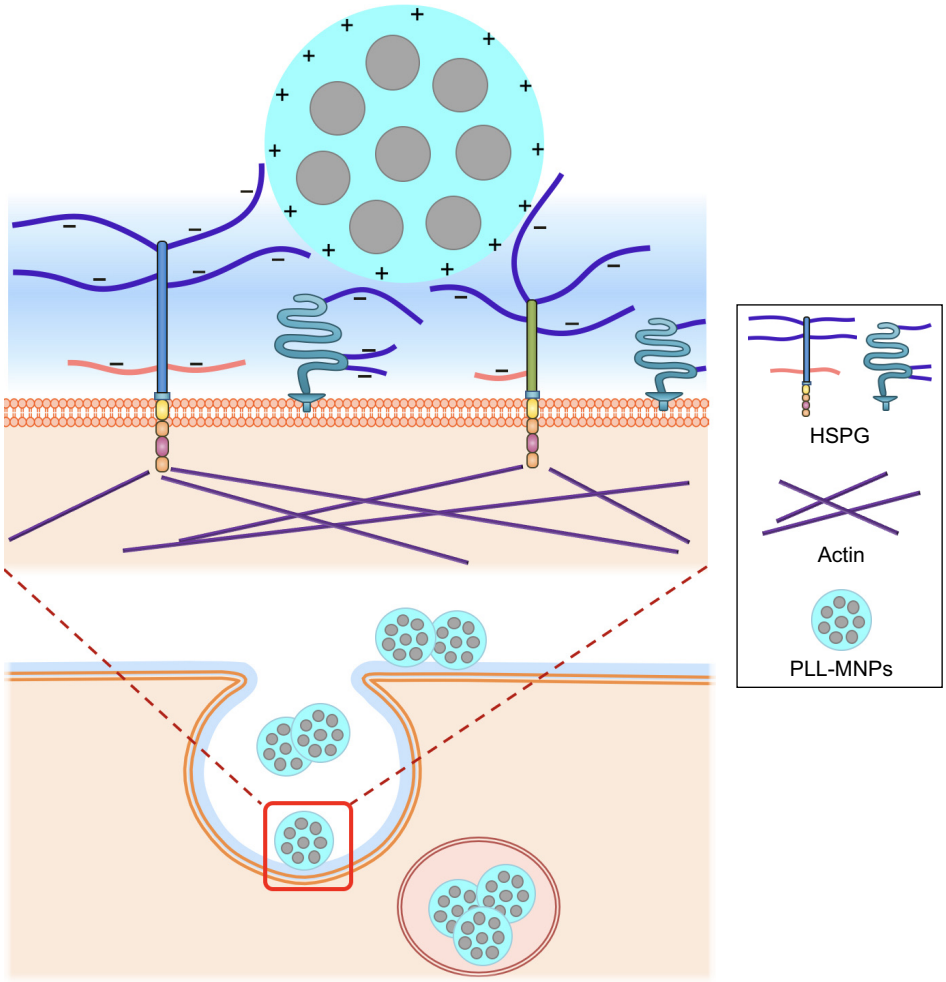

Figure 9 Schematic diagram of the interaction of PLL-MNPs and HSPG on the cell surface.
Notes: The amino groups of PLL coating endow positively charged residue (+) on the NP surface and interact with negatively charged residues (–) of heparan sulfate on cell surface. The upper diagram is an amplification of the red square in the lower diagram.
Abbreviations: PLL, poly-L-lysine; MNPs, magnetic nanoparticles; HSPG, heparan sulfate proteoglycan.

MNPs, as depicted in Figure 9. Such electrostatic interaction does not require application of magnetic force to maximize MNP uptake in tumor cells. In contrast, application of magnetic force in the presence of PLL may reduce MNP uptake. To our knowledge, this study is the first to provide the molecular mechanism of the effects of PLL on NP–cell interaction.

Our results indicated that both free and immobilized PLL greatly enhanced MNP uptake by glioma cells, which is consistent with previous findings that PLL enhanced NP internalization by stem cells[13,15–17,19] and other cells.[11,14,16–18,21] TEM results demonstrated microvilli formation associated with MNP internalization, suggesting that endocytosis may involve macropinocytosis,[20] which is usually the internalization pathway of particles >200 nm.[46] In our study, the number of internalized PLL-MNPs was much lower than Dex-MNPs with PLL in the culture medium, which was probably due to the smaller quantity of immobilized PLL. Since MNP_{cell} remained relatively high in the presence of PLL at 4°C, PLL is likely to enhance MNP interaction with plasma membrane. Furthermore, the coexistence of PLL and MNPs is imperative for enhanced MNP_{cell}, whereas preexposure to PLL was not required for the enhancement, suggesting that free PLL may interact with both MNPs and the moieties on the cell surface to facilitate MNP internalization.

In the absence of the magnet, the enhancing effects of PLL were associated with increased vesicle size and numbers of vesicle/cell (Figure 2), suggesting PLL–MNP interaction may occur and thus increase the separation distance between MNPs prior to endocytosis. PLL-coating-induced increase in MNP_{cell} was attenuated by the addition of EGCG (Figure 6), suggesting that positively charged amino groups of PLL may

be neutralized by negatively charged residues of EGCG, such as the hydroxyl groups of the phenolic structure. Amino groups of PLL appear to be required in its interaction with anionic molecules on the cell membrane and enhanced MNP_{cell}. Similar to EGCG, Hep attenuated the enhancing effect of PLL-coating on MNP internalization by glioma cells in a concentration-dependent manner. Our results suggest that PLL interacts directly with Hep or HS on the cell surface. In addition, MNP_{cell} with free PLL or PLL-coating was relatively low in HUVECs, which is consistent with previous finding that the expression level of HSPG is much lower in HUVECs.[47] The presence of Hep in culture media of HUVEC may partly compromise the effect of PLL, but MNP_{cell} of HUVECs still remained lower than that of cancer cells in Hep-free medium. In contrast to the lack of enhancing effects of the magnet on PLL-MNP internalization by glioma cells (Figure 4), significant magnetic effects were observed in HUVECs (Figure 8C and D), which is probably due to lower expression of HSPG in HUVECs. Although negatively charged, sialic acid moieties on the plasma membrane are unlikely to be involved in PLL-mediated MNP internalization. However, we cannot exclude other proteins or glycolipids present on the cell surface, which may participate or modulate PLL-mediated NP internalization, such as the transferrin receptor.[48]

Although a synergistic effect on MNP uptake was demonstrated with EGCG and magnetic force,[38] PLL and magnetic force exerted no synergistic effect on MNP internalization by glioma cells. It is plausible that PLL interacted chemically with Dex-MNPs and subsequently enhanced interaction of MNPs with the plasma membrane, which is consistent with the finding that PLL coating and magnetic force exerted no synergistic effect on PLL-MNP internalization. In addition, magnetic force significantly suppressed PLL-induced increase in MNP_{cell}, which is probably due to magnetic force-induced particle aggregation that reduced the surface area of particles to interact with HSPG on the surface of the cells. The proposed mechanism of PLL is further supported by the observation that vesicle size was greatly reduced in the presence of the magnet. Therefore, a fully exposed structure of PLL may be required in the interaction of MNPs with HSPG on the cell surface. With much lower levels of PLL-MNP internalization, the magnetic field failed to facilitate more internalization, suggesting that lack of magnet sensitivity may be independent upon levels of internalization. The applied magnetic force may also interfere with PLL–HSPG interaction that is secondary to aggregation, resulting in reduced MNP_{cell} (Figure 3). Alternatively, magnetic force-induced MNP agglomeration may reduce the number of amino groups of PLL available for interaction with the negatively charged macromolecules on the cell surface. Recently, reduced cellular internalization in magnetic field was also observed in MNPs of different sizes by different cells.[49,50]

Although EGCG attenuated the enhancing effect of PLL, this phenomenon was recovered after application of magnetic force. The typical EGCG-enhancing effect emerged in a concentration-dependent manner, suggesting that the positively charged amino groups of PLL interacted with hydroxyl groups of EGCG, resulting in restoration of the synergetic effects of EGCG with the magnetic force. Therefore, EGCG-induced endocytosis might be mediated by a different molecular mechanism from that mediated by PLL. Whether EGCG interacts with a 67 kDa laminin receptor[42,43,51] to enhance MNP internalization remains to be determined.

The endocytosis process per se is a consequence of force interaction,[2,52] and the magnetic-field gradient provides a downward force and thus facilitates endocytosis. Theoretical calculations based on consideration of the induced magnetic moment and magnet-field strength reveal an attractive force in pico-Newton range between the MNP and the membrane.[53] Since glycoconjugates located on cell surfaces contain components like GAG with dense anionic residues, it is anticipated that cationic polymers may interact with such negatively charged residues.[28] Based on the fluid mosaic model,[54] it is plausible that glycoconjugates with anionic residues build up a "charged network" on the cell surface, which may serve as a cushion in the extracellular milieu that provides an upward support against the magnetic downward force. By interaction with residues of glycoconjugates, PLL coating allows MNPs to overcome magnetic force-induced pulling of the particles toward the lipid bilayer, thus causing magnet insensitivity.

Conclusion

We demonstrated that the charged functional groups of PLL on the NP surface but not ζ-potential played a critical role in NP internalization by tumor cells. The amino groups of PLL selectively interacted with negatively charged, membrane-associated residues of glycoconjugates (Figure 9); the subsequent entanglement of the PLL with macromolecules at the surface milieu may hinder magnetic force to enhance MNP uptake further by these cells. In addition, magnetic force-induced MNP aggregation may impede interaction of the PLL coating with glycoconjugates. Therefore, surface modification of the MNPs may determine magnetic sensitivity

during magnetofection. With much less effect of PLL on the vascular endothelium, PLL-MNPs may potentially serve as drug carriers in targeting tumors that are inaccessible for magnetic targeting.

Acknowledgments

The authors thank Dr Albert M Wu, Graduate Institute of Biomedical Sciences, College of Medicine, Chang Gung University, for constructive suggestions regarding experimental design. We also appreciate Dr Timothy Wiedmann, Department of Pharmaceutics, College of Pharmacy, University of Minnesota, for critical reading of the manuscript. This work was supported by a Czech–Taiwanese project (Czech Science Foundation 16-01128J and MOST 105-2923-B-182-001-MY3) and Chang Gung University (CMRPD1D0231; BMRP432).

Disclosure

The authors report no conflicts of interest in this work.

References

1. Hoshyar N, Gray S, Han H, Bao G. The effect of nanoparticle size on in vivo pharmacokinetics and cellular interaction. *Nanomedicine (Lond)*. 2016;11(6):673–692.
2. Zhang S, Gao H, Bao G. Physical principles of nanoparticle cellular endocytosis. *ACS Nano*. 2015;9(9):8655–8671.
3. Zhu L, Zhou Z, Mao H, Yang L. Magnetic nanoparticles for precision oncology: theranostic magnetic iron oxide nanoparticles for image-guided and targeted cancer therapy. *Nanomedicine (Lond)*. 2016;12(1):73–87.
4. Singh D, McMillan JM, Kabanov AV, Sokolsky-Papkov M, Gendelman HE. Bench-to-bedside translation of magnetic nanoparticles. *Nanomedicine (Lond)*. 2014;9(4):501–516.
5. Estelrich J, Escribano E, Queralt J, Busquets MA. Iron oxide nanoparticles for magnetically-guided and magnetically-responsive drug delivery. *Int J Mol Sci*. 2015;16(4):8070–8101.
6. Lu YC, Chang FY, Tu SJ, Chen JP, Ma YH. Cellular uptake of magnetite nanoparticles enhanced by NdFeB magnets in staggered arrangement. *J Magn Magn Mater*. 2017;427:71–80.
7. Ulbrich K, Holá K, Šubr V, Bakandritsos A, Tuček J, Zbořil R. Targeted drug delivery with polymers and magnetic nanoparticles: covalent and noncovalent approaches, release control, and clinical studies. *Chem Rev*. 2016;116(9):5338–5431.
8. Khan MA, Wu VM, Ghosh S, Uskoković V. Gene delivery using calcium phosphate nanoparticles: optimization of the transfection process and the effects of citrate and poly(l-lysine) as additives. *J Colloid Interf Sci*. 2016;471:48–58.
9. Jin H, Yu Y, Chrisler WB, Xiong Y, Hu D, Lei C. Delivery of microRNA-10b with polylysine nanoparticles for inhibition of breast cancer cell wound healing. *Breast Cancer (Auckl)*. 2012;6:9–19.
10. Askarian S, Abnous K, Taghavi S, Oskuee RK, Ramezani M. Cellular delivery of shRNA using aptamer-conjugated PLL-alkyl-PEI nanoparticles. *Colloids Surf B Biointerfaces*. 2015;136:355–364.
11. Wang X, Zhang H, Jing H, Cui L. Highly efficient labeling of human lung cancer cells using cationic poly-L-lysine-assisted magnetic iron oxide nanoparticles. *Nano Micro Lett*. 2015;7(4):374–384.
12. Wang X, Wei F, Liu A, et al. Cancer stem cell labeling using poly(L-lysine)-modified iron oxide nanoparticles. *Biomaterials*. 2012;33(14):3719–3732.
13. Babič M, Horák D, Trchová M, et al. Poly(L-lysine)-modified iron oxide nanoparticles for stem cell labeling. *Bioconjug Chem*. 2008;19(3):740–750.
14. Babič M, Schmiedtová M, Poledne R, Herynek V, Horák D. In vivo monitoring of rat macrophages labeled with poly(L-lysine)-iron oxide nanoparticles. *J Biomed Mater Res B Appl Biomater*. 2015;103(6):1141–1148.
15. Mishra SK, Khushu S, Gangenahalli G. Potential stem cell labeling ability of poly-L-lysine complexed to ultrasmall iron oxide contrast agent: an optimization and relaxometry study. *Exp Cell Res*. 2015;339(2):427–436.
16. Frank JA, Miller BR, Arbab AS, et al. Clinically applicable labeling of mammalian and stem cells by combining superparamagnetic iron oxides and transfection agents. *Radiology*. 2003;228(2):480–487.
17. Arbab AS, Bashaw LA, Miller BR, et al. Characterization of biophysical and metabolic properties of cells labeled with superparamagnetic iron oxide nanoparticles and transfection agent for cellular MR imaging. *Radiology*. 2003;229(3):838–846.
18. Han G, Wu S, Wang J, Geng X, Liu G. Poly-L-lysine mediated synthesis of gold nanoparticles and biological effects. *J Nanosci Nanotechnol*. 2015;15(9):6503–6508.
19. Albukhaty S, Naderi-Manesh H, Tiraihi T. In vitro labeling of neural stem cells with poly-L-lysine coated super paramagnetic nanoparticles for green fluorescent protein transfection. *Iran Biomed J*. 2013;17(2):71–76.
20. Pongrac IM, Dobrivojević M, Ahmed LB, et al. Improved biocompatibility and efficient labeling of neural stem cells with poly(L-lysine)-coated maghemite nanoparticles. *Beilstein J Nanotechnol*. 2016;7:926–936.
21. Riggio C, Calatayud MP, Hoskins C, et al. Poly-L-lysine-coated magnetic nanoparticles as intracellular actuators for neural guidance. *Int J Nanomedicine*. 2012;7:3155–3166.
22. Heng BC, Cowan CM, Davalian D, et al. Electrostatic binding of nanoparticles to mesenchymal stem cells via high molecular weight polyelectrolyte chains. *J Tissue Eng Regen Med*. 2009;3(4):243–254.
23. Bush CA, Martin-Pastor M, Imberty A. Structure and conformation of complex carbohydrates of glycoproteins, glycolipids, and bacterial polysaccharides. *Annu Rev Biophys Biomol Struct*. 1999;28:269–293.
24. Dreyfuss JL, Regatieri CV, Jarrouge TR, Cavalheiro RP, Sampaio LO, Nader HB. Heparan sulfate proteoglycans: structure, protein interactions and cell signaling. *An Acad Bras Cienc*. 2009;81(3):409–429.
25. Mythreye K, Blobe GC. Proteoglycan signaling co-receptors: roles in cell adhesion, migration and invasion. *Cell Signal*. 2009;21(11):1548–1558.
26. Lin X. Functions of heparan sulfate proteoglycans in cell signaling during development. *Development*. 2004;131(24):6009–6021.
27. Christianson HC, Belting M. Heparan sulfate proteoglycan as a cell-surface endocytosis receptor. *Matrix Biol*. 2014;35:51–55.
28. Zarska M, Novotny F, Havel F, et al. Two-step mechanism of cellular uptake of cationic gold nanoparticles modified by (16-mercaptohexadecyl)trimethylammonium bromide. *Bioconjug Chem*. 2016;27(10):2558–2574.
29. Belting M. Heparan sulfate proteoglycan as a plasma membrane carrier. *Trends Biochem Sci*. 2003;28(3):145–151.
30. Cheng MJ, Kumar R, Sridhar S, Webster TJ, Ebong EE. Endothelial glycocalyx conditions influence nanoparticle uptake for passive targeting. *Int J Nanomedicine*. 2016;11:3305–3315.
31. Nasimuzzaman M, Persons DA. Cell membrane-associated heparan sulfate is a receptor for prototype foamy virus in human, monkey, and rodent cells. *Mol Ther*. 2012;20(6):1158–1166.
32. Jones KS, Petrow-Sadowski C, Bertolette DC, Huang Y, Ruscetti FW. Heparan sulfate proteoglycans mediate attachment and entry of human T-cell leukemia virus type 1 virions into $CD4^+$ T cells. *J Virol*. 2005;79(20):12692–12702.
33. Urbinati C, Nicoli S, Giacca M, et al. HIV-1 Tat and heparan sulfate proteoglycan interaction: a novel mechanism of lymphocyte adhesion and migration across the endothelium. *Blood*. 2009;114(15):3335–3342.

34. Tyagi M, Rusnati M, Presta M, Giacca M. Internalization of HIV-1 tat requires cell surface heparan sulfate proteoglycans. *J Biol Chem*. 2001; 276(5):3254–3261.
35. Connell BJ, Lortat-Jacob H. Human immunodeficiency virus and heparan sulfate: from attachment to entry inhibition. *Front Immunol*. 2013;4:385.
36. Wang H, Ma J, Yang Y, Zeng F, Liu C. Highly efficient delivery of functional cargoes by a novel cell-penetrating peptide derived from SP140-like protein. *Bioconjug Chem*. 2016;27(5):1373–1381.
37. Somiya M, Liu Q, Yoshimoto N, et al. Cellular uptake of hepatitis B virus envelope L particles is independent of sodium taurocholate cotransporting polypeptide, but dependent on heparan sulfate proteoglycan. *Virology*. 2016;497:23–32.
38. Lu YC, Luo PC, Huang CW, et al. Augmented cellular uptake of nanoparticles using tea catechins: effect of surface modification on nanoparticle-cell interaction. *Nanoscale*. 2014;6(17):10297–10306.
39. Kim HS, Quon MJ, Kim JA. New insights into the mechanisms of polyphenols beyond antioxidant properties; lessons from the green tea polyphenol, epigallocatechin 3-gallate. *Redox Biol*. 2014;2:187–195.
40. Afzal M, Safer AM, Menon M. Green tea polyphenols and their potential role in health and disease. *Inflammopharmacology*. 2015;23(4): 151–161.
41. Singh BN, Shankar S, Srivastava RK. Green tea catechin, epigallocatechin-3-gallate (EGCG): mechanisms, perspectives and clinical applications. *Biochem Pharmacol*. 2011;82(12):1807–1821.
42. Fujimura Y, Sumida M, Sugihara K, Tsukamoto S, Yamada K, Tachibana H. Green tea polyphenol EGCG sensing motif on the 67-kDa laminin receptor. *PLoS One*. 2012;7(5):e37942.
43. Tachibana H, Koga K, Fujimura Y, Yamada K. A receptor for green tea polyphenol EGCG. *Nat Struct Mol Biol*. 2004;11(4):380–381.
44. Christianson HC, Svensson KJ, van Kuppevelt TH, Li JP, Belting M. Cancer cell exosomes depend on cell-surface heparan sulfate proteoglycans for their internalization and functional activity. *Proc Natl Acad Sci U S A*. 2013;110(43):17380–17385.
45. Kou L, Sun J, Zhai Y, He Z. The endocytosis and intracellular fate of nanomedicines: implication for rational design. *Asian J Pharmacol*. 2013; 8:1–10.
46. Sigismund S, Confalonieri S, Ciliberto A, Polo S, Scita G, Di Fiore PP. Endocytosis and signaling: cell logistics shape the eukaryotic cell plan. *Physiol Rev*. 2012;92(1):273–366.
47. Hu Q, Kang T, Feng J, et al. Tumor microenvironment and angiogenic blood vessels dual-targeting for enhanced anti-glioma therapy. *ACS Appl Mater Interfaces*. 2016;8(36):23568–23579.
48. Li Z, Shuai C, Li X, Li X, Xiang J, Li G. Mechanism of poly-L-lysine-modified iron oxide nanoparticles uptake into cells. *J Biomed Mater Res A*. 2013;101(10):2846–2850.
49. Katebi S, Esmaeili A, Ghaedi K. Static magnetic field reduced exogenous oligonucleotide uptake by spermatozoa using magnetic nanoparticle gene delivery system. *J Magn Magn Mater*. 2016;402:184–189.
50. Shanehsazzadeh S, Lahooti A, Hajipour MJ, Ghavami M, Azhdarzadeh M. External magnetic fields affect the biological impacts of superparamagnetic iron nanoparticles. *Colloids Surf B Biointerfaces*. 2015; 136:1107–1112.
51. Wang QM, Wang H, Li YF, et al. Inhibition of EMMPRIN and MMP-9 expression by epigallocatechin-3-gallate through 67-kDa laminin receptor in PMA-induced macrophages. *Cell Physiol Biochem*. 2016; 39(6):2308–2319.
52. Pyrgiotakis G, Blattmann CO, Demokritou P. Real-time nanoparticle-cell interactions in physiological media by atomic force microscopy. *ACS Sustain Chem Eng*. 2014;2(7):1681–1690.
53. Furlani EP, Xue X. Field, force and transport analysis for magnetic particle-based gene delivery. *Microfluid Nanofluidics*. 2012;13(4): 589–602.
54. Nicolson GL. The fluid-mosaic model of membrane structure: still relevant to understanding the structure, function and dynamics of biological membranes after more than 40 years. *Biochim Biophys Acta*. 2014; 1838(6):1451–1466.